Rockfall monitoring: comparing several strategies for surveying detached blocks and their volume, from TLS point clouds and GigaPan pictures

Oriol Pedraza[1], Álvaro P. Aronés[2], Càrol Puig[2], Marc Janeras[1], Josep A. Gili[2]

[1] Institut Cartogràfic i Geològic de Catalunya, Barcelona, Spain, (oriol.pedraza@icgc.cat; marc.janeras@icgc.cat)
[2] Universitat Politècnica Catalunya, Barcelona, Spain, (apauloav@hotmail.com; carol.puig@upc.edu; j.gili@upc.edu)

Key words: *rockfall; change detection; C2M; M3C2; Terrestrial Laser Scanning; geomatic techniques*

ABSTRACT

Rockfalls are fast slope instabilities frequent in mountainous areas, which cause damage in infrastructures (roads and railways), buildings, vehicles and people. Nowadays, several continuous and discontinuous techniques are available to monitoring the prone areas in order to manage the associated risk. One side task is to detect changes in the source zones (rock cliffs with recurrent events) in order to assess the rockfall activity and calibrate the Magnitude-Frequency curves. Long range and high precision Terrestrial Laser Scanning (TLS) is currently used for this purpose, sometimes in combination with high-resolution pictures taken from UAV or from the ground (with a GigaPan setup, for instance). Some detected changes along time may correspond to precursory displacements while others are due to blocks detached from the cliffs. In our contribution, we present the use of the aforementioned geomatic techniques (TLS and GigaPan) within several algorithms /strategies (Cloud to Cloud, Cloud to Mesh and M3C2) inside some two commercial computer programs and open source program in order to detect and measure the differences along the successive field campaigns. This work has being carried out within the frame of the GeoRisk research project, with field data from the ICGC. In particular, we test the strategies in three sites in the Montserrat Massif (Spain) –Mirador de l'Oliver, Canal dels Aritjols and Mirador dels Apòstols– during four measuring epochs along 2019-2021. The results show that rock volumes as small as 0.001 m³ can be detected in a regular basis.

I. Introduction

Service and transport infrastructures located in mountainous and steep terrain could be exposed to various landslide hazards, including rockfalls. Rockfall is characterized as a fragment or fragments of rock which detach from a cliff face and, subsequently, fall, bounce, and roll as the fragments propagate downslope (Hungr *et al*., 2014). Although their magnitude can be highly variable, rockfalls cause frequent damage due to their intensity and frequency, both temporally and spatially. This poses a major challenge when prioritising the allocation of resources for landslide risk mitigation over large areas.

A clear example is the Montserrat massif (Spain), which constitutes a Natural Park (about 3500 ha) and hosts a monastery with a millenarian history and great tradition in Catalonia. Combining local and foreign tourism, the number of visitors to the monastery area was 2.7 million in 2017, with a further 0.8 million people travelling through the Natural Park for hiking or climbing.

Quantitative rockfall risk analysis (QRA) allows us to assess the different risk scenarios present in infrastructures (Corominas *et al*., 2005). This quantification is obtained by developing magnitude-frequency relationships from inventory of events, where the cumulative frequency is quoted in spatial and temporal terms (Janeras *et al*., 2021).

The magnitude-frequency relationships are obtained through known rockfall events. However, some bias on the information on events (mainly the lack of high magnitude and low frequency records) can lead to inaccurate quantification of risk. To partially overcome this situation, in the last decade Terrestrial Laser Scanning (TLS) and/or digital photogrammetry monitoring have complemented this lack of information with site-specific sampling and increased detection capacity (Royán, 2015; Van Veen *et al.*, 2017).

In our contribution, we present the use of the TLS and GigaPan combined with several algorithms/strategies (Cloud to Cloud, Cloud to Mesh, M3C2) in order to detect and measure the differences along the successive field campaigns over the rock cliffs. In particular, we test the techniques in three test sites in the Montserrat Massif (Spain) during four measuring epochs along 2019-2020.

II. Study site and objectives

The mountain of Montserrat is located 50 km northwest of the city of Barcelona in Catalonia, in the extreme northeast of Spain (Figure 1). This isolated massif, formed by thick conglomerate layers interspersed by siltstone/sandstone from a late Eocene fan-delta, emerges above the Llobregat river with a total height of 1000 m (from 200 to 1200 m a.s.l.).
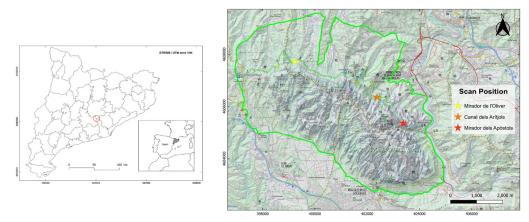
Figure 1. Site map of Montserrat massif, 50 km NW Barcelona city (Catalonia, Spain). The massif ranges between 200 and 1200 m a.s.l. over the Llobregat river at the East. The image shows the three stations where terrestrial laser scanning has been carried out.

Because of the process of sedimentation and the tectonic stresses, the massif is constituted by an intercalation of conglomerate and fine layers of sandstone and siltstone affected by a few joint sets, the prevailing two main near-vertical sets following direction NE-SW and NO-SE, respectively (Alsaker *et al.*, 1996). This configuration gives rise to stepped slopes where vertical cliffs alternate with steep slopes.

The joint systems present and their density, define the blocks susceptible to fall and therefore control the size of the blocks and the magnitude of the rockfalls. From lower to higher volume, it starts with the disaggregation of pebbles from the conglomerate (M3); as the second group (M2) we distinguish the slabs and plates related to physical weathering; and finally, monolithic rock masses delimited by widely spaced joints with very high persistence, (M1) (Janeras *et al.*, 2017).

The main objective of this work is to assess the suitability of the aforementioned geomatic techniques (TLS and GigaPan) to detect and quantify the rockfall events that may occur in three study sites in the period 2019-2021. The sites in this study will be named as follows: [i] Mirador de l'Oliver, [ii] Canal dels Arítjols and [iii] Mirador dels Apòstols. Two of the study sites were located on the BP-1103 road, being the third one close to the Montserrat monastery (Figure 1).

The study was carried out with three TLS point cloud processing software packages, comparing the detected rockfall with the two methods of change detection used.

III. Monitoring strategy and systems

The Montserrat massif is under progressive surveillance with a wide range of methods, which are described in Janeras *et al*. (2017). From manual and point-based techniques to automatic and continuous systems are in use in the whole area in order to manage the high geological risk over the infrastructures and the visitors. As previously stated, the TLS and the photomonitoring are techniques tested in this study

because they offer a good balance between spatial & time continuity, precision and feasibility. In the following Section A and B, we describe the main characteristics of these techniques as applied in our study.

On the other hand, in the last decade automated and semi-automated workflows have been developed to process the TLS datasets (point clouds), so that professionals can spend more time analysing and interpreting the field net results. Therefore, comparing successive TLS point clouds, the algorithms might detect the changes of the cliff surface, which can be associated as blocks detached from source areas. The volume of these masses are of paramount importance for deriving Magnitude-Frequency relationships.

The present study focuses on testing the most used change detection methods, described in Section C, in order to assess their suitability for the detection of detached blocks in practice.

A. *Terrestrial laser scanning for rockfall monitoring*

LiDAR technology is a remote sensing method used to acquire terrain information in the form of point clouds; a collection of data points in three-dimensional (3D) space. Using a terrestrial laser scanner (TLS) we can rapidly measure the reflected energy of an emitted laser pulse (Girardeau-Montaut *et al*., 2005), thus acquiring detailed point clouds of terrain with very precise measurements of surface geometry. In the last decade, TLS has become a routine data source for rock slope characterisation and monitoring, especially for its effectiveness in capturing oblique views of vertical rock slopes (Barnhart and Crosby, 2013).

Rockfall detection from the comparison of two-point clouds obtained by LiDAR has been widely used and reported in different articles around the world. In this sense, the Montserrat mountain is not an exception and several authors have carried out their academic work, generating several lines of research started by Abellán (2009) and followed by Royán (2015), Blanch (2016), García (2018), Vinueza (2020), Arones (2021) and Blanco *et al.* (2021).

The technical spec of the TLS sensor and the terrain condition influence the error in the gathered points. According to Jaboyedoff *et al. (*2012) the most relevant sensor parameters are: the laser wavelength; the range measurement method (related to the range precision); the maximum range at select target reflectivity; the laser footprint; and the minimum horizontal and vertical angular increment. The LiDAR equipment is being improved year by year, and as a result, nowadays we are able to capture data faster, at higher densities and precision (Lague *et al.*, 2013).

In the present study, we have used a Leica ScanStation P50 time-of-flight system (Figure 2).

Figure 2. TLS used in the study, Leica ScanStation P50. In the background, the characteristic Montserrat landscape can be appreciated: stepped slopes where vertical conglomerate intercalation of and fine layers of sandstone and siltstone.

The maximum range of Leica P50 depends on the object/terrain reflectivity (Table 1). The precision is remarkable even at these medium/long scanning distances.

Table 1. Leica ScanStation P50 range and precision

TLS System	Max Range	Precision in range	Object Reflectivity
Leica ScanStation P50	270 m	1.2 mm + 10 ppm	34%
	570 m	3 mm + 10 ppm	60%

B. *GigaPan*

High-resolution panoramic images were generated from a series of pictures captured during each field campaign to aid interpretation of the TLS data. The high-resolution photographs were taken from the scanning position using a Nikon D5300 full frame 24.2 megapixel camera, with a NIKKOR AF-S DX 18-140mm f/3.5-5.6G ED VR - Nikon lens. The camera was mounted on a GigaPan EPIC PRO motorised panoramic head (Figure 3), produced by GigaPan Systems LLC (Lato *et al.*, 2012). The photos were stitched together using GigaPan Stitch software, resulting in a seamless high-resolution panoramic photo of the rock slope (Figure 4).

C. *Methods of Change Detection*

Change detection analyses using TLS data are difficult because of (1) the complexity and richness of the point clouds representing the natural environment and (2) because TLS point clouds from different temporal epochs or physical scan positions may not overlap closely enough for accurate point to point comparison (Barnhart and Crosby, 2013). Additionally, the software packages used to process TLS data are often optimized for the built environment and lack analytical tools relevant to natural landscapes.

However, some change detection methods have been successfully used to capture surface changes caused by geomorphic processes, each with their respective advantages and disadvantages. The most commonly used are the following: Cloud-to-Cloud (C2C), Cloud-to-Mesh (C2M), and Multiscale Model-to-Model Cloud Comparison (M3C2). The C2C method compares the points of the first cloud directly with the closest one on the second cloud. In general, the results with C2C are quite noisy, especially when the terrain has some roughness. Therefore, we decide to use and compare the performance of the C2M and M3C2 methods, which are summarized in the next two subsections.

1) C2M method: The Cloud to Mesh (C2M) distance comparisons have been used by many authors to detect a change between successive point clouds (Abellán *et al.*, 2009; 2010; Guerin *et al.*, 2014; Vinueza, 2020). To use the C2M algorithm it is necessary to create a reference (or baseline) mesh, which was built with the point cloud corresponding to the first campaign (July 2019). The algorithm needs at least the following parameters: the size of the triangles for the triangulation of the points and the average distance of the points. The interpolation between the clouds of reference points for the creation of the facets of a triangulated surface model is a complex computational process with irregular surfaces, especially if they have significant roughness. C2M calculates the distance from each point of the second cloud to the nearest point of a facet of a triangulated surface model of the reference cloud (Figure 5A). The accuracy of C2M depends on how well the surface mesh can model the terrain without over interpolating the original geometry of the input point cloud.

Figure 3. GigaPan Epic Pro robotic head with screen and controls equipped with a Nikon D5300 camera.
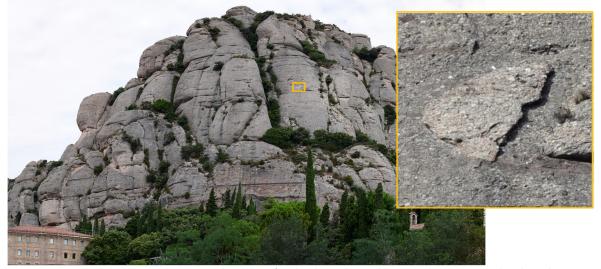
Figure 4. Gigapixel panoramic image, Mirador dels Apòstols. The High Resolution can be appreciated in the right inset.
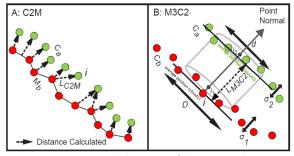

Figure 5. Conceptual diagrams of the C2M and M3C2 techniques. Both A and B are modified from Barnhart *et al.* (2013).

2) M3C2 Method: The multiscale model-to-model cloud comparison (M3C2) algorithm created by Lague *et al.* (2013) measures the distance along a local normal vector estimated from each point's neighbourhood, and thus considers local surface orientation in the distance computations. The algorithm projects search cylinders along the local normal vectors to find the locally averaged change between the two clouds. The M3C2 requires two user-defined parameters, which are the normal scale and the projection scale. The normal scale (D) is based on the density and roughness of the reference point cloud and is the diameter around each central point to calculate a local normal. The projection scale (d) is used to calculate the distance between the two-point clouds and is determined by the defined radius and length of a projection cylinder (Figure 5B). The algorithm operates directly on the point clouds and therefore does not require meshes or grids.

In this study and considering the values reported by Garcia (2018) and Di Francesco *et al.* (2020), the following parameters have been used: the value of 0.25 m has been chosen, since the average distance between the points of the scans is 0.1 m; therefore, between 7 and 8 points of the scan will be used to calculate the normal. This is adequate to avoid too great an influence of the dispersion of points due to the

instrumental error without losing the detail of the real roughness of the surface studied.

IV. ACQUIRED DATA

The terrestrial laser scanning was carried out at the three sites described in II, two scans per year, from July 2019 to December 2020. The campaigns or epochs will be named as summarized in Table 2.

Table 2. Campaigns T0-T3

Field date	Name
July 2019	T0 (reference)
December 2019	T1
July 2020	T2
December 2020	T3

The same TLS system was used to collect data at all three sites during the 2-year monitoring period. Each survey consisted of at least one scanning position for each site, with a maximum distance of 375 m and a minimum distance of 75 m from the survey wall.

Figure 6 shows the extent of one of the scan areas. Leica ScanStation P50 scans were parsed using Leica *Cyclone REGISTER 360* software.
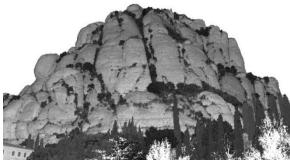

Figure 6. Example of the area covered by July 2019 (T0) scan at the Mirador dels Apòstols.

V. ANALYSIS OF RESULTS. COMPARISON OF METHODS

The rockfall extraction process is depicted in Figure 7. Change detection was conducted to outline active areas due to rockfall.
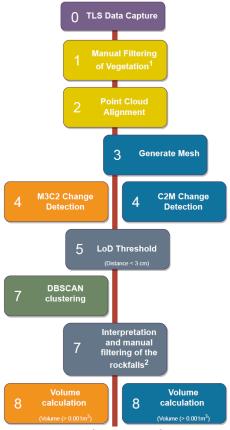

Figure 7. Rockfall detection flowchart.

Point cloud processing has been performed independently with three computer programs: CloudCompare (Girardeau-Montaut, 2021), PointStudio (Maptek, 2021) and Cyclone 3DR (Leica, 2021).

Each software has different tools for the comparison of point clouds and the detection of possible rockfalls (Table 3). Depending on whether point clouds or surfaces are compared, different tools are used.

Table 3. Algorithms in use

Software	Algorithm
Pointstudio (Maptek)	C2M
Cyclone 3DR (Leica)	C2M
CloudCompare	C2M and M3C2

Vegetation was manually removed from the raw point clouds and with the cleaned point clouds aligned to the July 2019 baseline. For the alignment of the clouds, different algorithms are available for each software.

Firstly, with the CloudCompare and Leica Cyclone 3DR software coarse alignment was carried out by manually selecting a minimum of 4 points from the stable areas of the slope with clearly identifiable geometry (Figure 8).

Figure 8. Data processing workflow.

However, with the Maptek PointStudio software, overlapping is achieved by selecting the clouds to be moved, working with the entire point cloud. Once the coarse alignment was done, it was followed by a fine alignment process. In the case of the CloudCompare software, it has the Iterative Closet Points (ICP) algorithm, which is based on aligning the clouds based on a set of strategic points that overlap each other. Similar algorithms are used in Maptek PointStudio and Cyclone 3DR software.

In the three software, records have been obtained in which a root mean square error (RMS) can be observed, with values of, approximately 6 cm. The RMS values of each cloud vary in each software. This variation is because each of them works with a different algorithm to perform the fine alignment process. However, the values are within the same range.

We use both C2M and M3C2 methods for the detection of changes due to rockfall. The change backwards in time highlights the fronts of the changing features. A detection limit threshold was used to extract the fronts and reversals of the loss features. Detection artefacts generated because of random noise within the TLS datasets were manually removed from the point cloud. Finally, false positives were filtered out using (1) a positive-to-negative point ratio threshold and (2) a minimum volume threshold.

The rockfalls detected using the methodology presented in this paper have been summarised in the following Table 4. A total of 8 rockfalls have been detected in the three sector which have been studied. In the Mirador de l'Oliver area, no rockfalls were detected in the period July 2019- December 2020 (T0-T3). In the Canal dels Arítjols area, 1 rockfall was detected in the period July - December 2019 (T0-T1). In the analysis of clouds T1-T2 and T2-T3 no detachments were detected. In the Mirador dels Apòstols area, 7 rockfalls were detected in the period July 2019 - July 2020 (T0-T2). Between T0-T1, there were 3 rockfalls; in the period T1-T2 there were 4 rockfalls and finally in the period T2-T3 no rockfalls were detected.

Table 4. Number of rockfalls --or detached blocks-- per site

Site	T0-T1	T1-T2	T2-T3	Total
Mirador de l'Oliver	0	0	0	0
Canal dels Arítjols	1	0	0	1
Mirador dels Apòstols	3	4	0	7

In the three software used and with the C2M algorithm, the same rockfalls have been detected in each sector (Figure 9 and Table 5). The detection of these rockfalls was carried out manually and corroborated with Gigapixel panoramic images (Figure 10). In the case of the M3C2 algorithm (CloudCompare), similar results were also obtained as can be seen in Figure 9 (right).
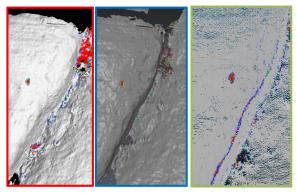

Figure 9. Example of a detached block detected with the three programs: PointStudio- C2M (left); Cyclone- C2M (center); CloudCompare –M3C2 (right).

Figure 10. Mirador dels Apòstols site. Comparison between Gigapixel images: T0 campaigns (pre-detachment, left) and T1 campaign (post-detachment, right). In red circle the detected detachment, with a volume of 0.001 m³.

Once the rockfalls detected, we computed their volume. Each software has different ways for that. In the case of Maptek PointStudio, the volume below a surface in relation plane orthogonal to visual TLS at a fixed elevation is calculated. With this method of calculation, it is necessary to analyse each scanned surface independently, the difference between surfaces giving the volume of detached rock (Vinueza, 2020). The Cyclone 3DR obtains the volumes on closed surfaces, so it must be ensured that the meshes containing the rockfall are free of voids that could affect the result. Finally, CloudCompare has the "2.5 D

Volume" volume calculation tool, which can calculate the volume between two clouds through a process of rasterization (gridding) of the point clouds.

The same rock falls have been detected in all three software packages and with both change detection methods, as they have been corroborated by the HR images (Figure 10), and the calculated volumes are relatively similar, even for such small volumes: For instance, the Table 5 shows that the volumes range from 0.001 to 0.055 m³, with detachments of less than 0.01 m³ predominating. The sum of the volumes of all detected rockfalls ranges from 0.078 m³ to 0.068 m³. It is important to mention that these small disparities may be due to differences in the procedure for calculating the volume. For this reason, not having detected any significant rockfall, we state that the instabilities occurring in the study sectors are of low magnitude for the period under consideration.

The Magnitude-Frequency graph corresponding to the 7 rockfalls found in the Mirador dels Apòstols is presented in the Figure 11.
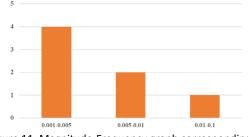

Figure 11. Magnitude-Frequency graph corresponding to the 7 rockfalls detected in the Mirador dels Apòstols.

In addition, satisfactory tests have been carried out with the DBSCAN algorithm to facilitate the detection of rockfalls. As discussed by Tonini and Abellán (2014), an adaptation of the Density-Based Spatial Clustering Algorithm for Noisy applications (DBSCAN) (Ester *et al.*, 1996) was used to cluster individual rockfall events from the unorganised input point cloud. We implemented out the DBSCAN algorithm using R software for statistical computing (R Development Core Team, 2012). R is a free software environment integrating facilities for data manipulation and calculation. The R base can be extended via packages available through the Comprehensive R Archive Network (CRAN).

Table 5. Mirador dels Apòstols, comparison of volumes measured with the C2M method with the three programs

Sector	Volumes measured with Cyclone 3DR [m³]				Volumes measured with Maptek Pointstudio [m³]				Volumes measured with Cloudcompare [m³]			
	N1-N2	N2-N3	N3-N4	Total	N1-N2	N2-N3	N3-N4	Total	N1-N2	N2-N3	N3-N4	Total
Zona 1	0.008	0.002	0	0.015	0.003	0.001	0	0.005	0.008	0.003	0	0.016
		0.005				0.001				0.003		
Zona 3	0	0.013	0	0.013	0	0.004	0	0.004	0	0.005	0	0.015
Zona 5	0.005	0.044	0	0.049	0.003	0.055	0	0.058	0.002	0.047	0	0.043
Zona 7	0.001	0	0	0.001	0.001	0	0	0.001	0.002	0	0	0.002
Total	**0.014**	**0.064**	**0**	**0.078**	**0.007**	**0.061**	**0**	**0.068**	**0.013**	**0.063**	**0**	**0.070**

The DBSCAN algorithm looks for sets of positive differences around a given point, according to some search parameters (minimum number of points and search radius) (Figure 12).
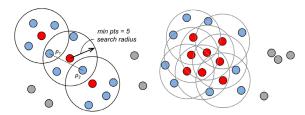

Figure 12. The DBSCAN algorithm there are three types of points as follows: key points (red) are points that satisfy the cluster criteria; border points (blue) do not satisfy the cluster criteria but are within a key point's reach; noise points (grey). From Di Francesco *et al.* (2020).

We started with those proposed in Royán (2015) and Blanch (2016). After a trial-and-error process, using datasets of different characteristics, we concluded that the minimum number of neighbours that the clusters must contain is 15, and the appropriate search radius is 0.01 m in our case.

The clustering process resulted in a point cloud of clustered objects, each with a unique ID. The results were visualised in CloudCompare (Figure 13). Only a small fraction of the clusters corresponds to rockfalls. Most of them are false positives due to the "edge effect" near the limits of the large rock sheets, or related with some remains of vegetation.
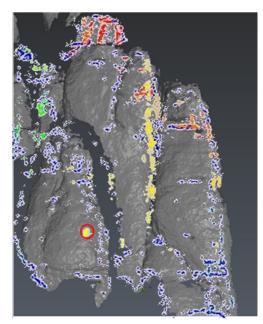

Figure 13. Example of the clusters obtained with DBSCAN. A confirmed rockfall can be appreciated within the red circle, being the rest 'false positives'.

VI. CONCLUSIONS

Rockfall inventories are essential for capturing rockfall activity and understanding the hazard. The inventories are the basis for the quantitative risk analysis because the Magnitude-Frequency curves permit the assignment of an annual probability of occurrence for each magnitude.

Our campaigns in Montserrat confirmed that TLS instruments enable a detailed monitoring of the rock cliffs, attaining a new level of accuracy and resolution. Our research shows that CloudCompare, PointStudio and Cyclone (with C2M and/or M3C2 change detection algorithms) offer very similar results for the covered area and period, even for volumes as small as 0.001 m³.

We conclude that the same methodology will give satisfactory results in the detection of larger rockfalls, M1 and M2 type, with volumes greater than 0.1 m³.

The biggest advantage of CloudCompare is its free licence, greater control of intermediate processes and choice of change detection algorithm, while PointStudio and Cyclone offer more automated processes. Although, according to recent literature, the M3C2 algorithm is more satisfactory and widely used than C2M, in this study we conclude that for complex and irregular surfaces both offer very similar and acceptable results.

In the workflow followed, there are certain tasks that are not automated. Vegetation filtering and rockfall checking on HR images are tedious and time-consuming manual steps. Additional work must be devoted to this automation before TLS monitoring can be truly productive. For instance, for automated rockfall extraction, the improvements may include: the incorporation of the normals (indicative of rock structure, to be used in M3C2); smart routines for clutter and artefact removal; further automation of change detection feature classification; and clustering algorithms capable of separating coalescing rockfall events.

On the other hand, the large number of events collected over years of monitoring will allow the use of Machine Learning techniques to improve the automatic classification of clusters (Blanco *et al*., 2021).

VII. ACKNOWLEDGEMENTS

References

Abellán, A. (2009). *Improvements in our understanding of rockfall phenomenon by Terrestrial Laser Scanning*. Emphasis on change detection and its application to spatial prediction. Universitat de Barcelona - PhD.

Abellán, A., Calvet, J., Vilaplana, J., and Blanchard, J. (2010). Detection and spatial prediction of rockfalls by means of terrestrial laser scanner monitoring. *Geomorphology*, 119, pp. 162–171.

Abellán, A., Jaboyedoff, M., Oppikofer, T., and Vilaplana, J. (2009). Detection of millimetric deformation using a terrestrial laser scanner: experiment and application to a rockfall event. *Natural Hazards and Earth System Science*, 9, pp. 365–372. DOI: 10.5194/nhess-9-365-2009

Alsaker, E., Gabrielsen, R.H., and Roca, E. (1996). The significance of the fracture patterns of Late-Eocene Montserrat fan-delta, Catalan Coastal Ranges (NE Spain), *Tectonophysics,* 266, pp. 465–491.

Arones, A. (2021). *Monitorización de desprendimientos rocosos en la Montaña de Montserrat mediante técnicas láser. Comparación de alternativas de procesado para la detección de bloques desprendidos*. (Trabajo Final de Máster). Universitat Politècnica de Catalunya, Barcelona.

Barnhart, T.B., and Crosby, B.T. (2013). Comparing Two Methods of Surface Change Detection on an Evolving Thermokarst Using High-Temporal-Frequency Terrestrial Laser Scanning, Selawik River, Alaska. *Remote Sens.,* 5, pp. 2813–2837.

Blanch, X. (2016). *Anàlisi estructural i detecció de despreniments rocosos a partir de dades LiDAR a la Muntanya de Montserrat*. (Trabajo Final de Grado). Universitat Politècnica de Catalunya, Barcelona.

Blanco, L., García-Sellés, D., Pascual, N., Puig, A., Salamó, M., Guinau, M., Gratacos, O., Muñoz, J.A., Janeras, M., and Pedraza O. (2021). Identificación y clasificación de desprendimientos de roca con LIDAR y machine learning en Montserrat y Castellfollit de la Roca (Cataluña). *X Congreso Geológico de España*, 5-7 Julio 2021. Vitoria-Gasteiz. España.

Corominas, J., Copons, R., Moya, J., Vilaplana, J. M., Altimir, J., and Amigo, J. (2005). Quantitative assessment of the residual risk in a rockfall protected area. *Landslides*, 2, pp. 343–357.

Di Francesco, P.-M., Bonneau, D., and Hutchinson, J. (2020). The Implications of M3C2 Projection Diameter on 3D Semi-Automated Rockfall Extraction from Sequential Terrestrial Laser Scanning Point Clouds. *Remote sensing*, 12, 27. DOI: 10.3390/rs12111885

Ester, M., Kriegel, H., Sander, J., and Xu, X. (1996). A Density-Based Algorithm for Discovering Clusters in Large Spatial Databases with Noise. In *Proceedings of the Second International Conference on Knowledge Discovery and Data Mining*, Portland, OR, USA, 2–4 August 1996; Simoudis, E., Fayyad, U., Han, J., Eds.; AAAI Press: Menlo Park, CA, USA, pp. 226–231.

Garcia, M. (2018). *Millora metodològica per a la detecció i caracterització de despreniments amb*. Trabajo de Fin de Máster. Universitat de Barcelona, Barcelona.

Girardeau-Montaut, D., Roux, M., Marc, R., Thibault, G. (2005). Change Detection on Point Cloud Data Acquired with a Ground Laser Scanner. *Int. Arch. Photogramm. Remote Sens. Spat. Inf. Sci.,* 36, pp. 30–35.

Girardeau-Montaut, D. (2021). CloudCompare, Version 2.11.3 Anoia. Available online: http://cloudcompare.org (accessed on 28 December 2021).

Guerin, A., Hantz, D., Rossetti, J.-P., and Jaboyedoff, M. (2014). Brief Communication: Estimating Rockfall Frequency in a Mountain Limestone Cliff Using Terrestrial Laser Scanner. *Nat. Hazards Earth Syst. Sci. Discuss*., 2, pp. 123–135.

Hungr, O., Leroueil, S., Picarelli, L., Article, R. (2014). The Varnes Classification of Landslide Types, an Update. Landslides, 11, pp. 167–194.

Jaboyedoff, M., Oppikofer, T., Abellán, A., Derron, M.H., Loye, A., Metzger, R., and Pedrazzini, A. (2012). Use of LIDAR in Landslide Investigations: *A Review. Nat. Hazards*, 61, pp. 5–28.

Janeras M., Jara, J.A., Royán, M.J., Vilaplana, J.M., Aguasca, A., Fàbregas, X., Gili, J.A., and Buxó, P. (2017). Multitechnique approach to rockfall monitoring in the Montserrat massif (Catalonia, NE Spain). *Engineering Geology*, 219 (2017) 4–20. DOI: 10.1016/j.enggeo.2016.12.010.

Janeras, M., Pedraza, O., Lantada, N., Hantz, D., and Palau, J. (2021). TLS - and inventory-based Magnitude - Frequency relationship for rockfall in Montserrat and Castellfollit de la Roca. Conference: *5th RSS Rock Slope Stability Symposium*, Chambéry, France.

Lague, D., Brodu, N., and Leroux, J. (2013). Accurate 3D Comparison of Complex Topography with Terrestrial Laser Scanner: Application to the Rangitikei Canyon (N-Z). *ISPRS J. Photogramm. Remote Sens*, 82, pp. 10–26.

Lato, M.J., Bevan, G., and Fergusson, M. (2012). Gigapixel Imaging and Photogrammetry: Development of a New Long Range Remote Imaging Technique. *Remote Sens*., 4, pp. 3006–3021.

Leica Geosystems AG (2021). Leica ScanStation P50 Product Specifications; Switzerland.

Leica Cyclone (2021). REGISTER 360-3D Laser Scanning Point Cloud Registration Software. Available online: https://leica-geosystems.com/products/laser-scanners/software/leica-cyclone/leica-cyclone-register-360 (accessed on 15 November 2021)

Maptek Pointstudio (2021). Software. Available online: h https://www.maptek.com/products/pointstudio/ (accessed on 15 November 2021)

Leica Cyclone (2021). 3DR Software. Available online: https://leica-geosystems.com/es-es/products/laser-scanners/software/leica-cyclone/leica-cyclone-3dr (accessed on 15 November 2021)

R Development Core Team (2012). R: A Language and Environment for Statistical Computing. R Foundation for Statistical Computing, Vienna, Austria, https://www.r-project.org/

Royán, MJ. (2015) *Caracterización y predicción de desprendimientos de rocas mediante LiDAR terrestre*. PhD Thesis, Vilaplana (Adv.) Universitat de Barcelona

Tonini, M., and Abellán, A. (2014). Rockfall Detection from Terrestrial LiDAR Point Clouds: A Clustering Approach Using R. *J. Spat. Inf. Sci.*, 2014, pp. 95–110

Van Veen, M., Hutchinson, D.J., Kromer, R., Lato, M., and Edwards, T. (2017). Effects of Sampling Interval on the Frequency-Magnitude Relationship of Rockfalls Detected from Terrestrial Laser Scanning Using Semi-Automated Methods. *Landslides*, 14, pp. 1579–1592.

Vinueza, J. R. (2020). *Monitoreo de bloques de rocas mediante el uso de láser escáner terrestre (TLS). Estudio de alternativas para la detección de bloques desprendidos*. Trabajo de Fin de Máster. Universitat Politècnica de Catalunya, Barcelona.